

Single-step transfer of biosynthetic operons endows a non-magnetotactic *Magnetospirillum* strain from wetland with magnetosome biosynthesis

Marina V. Dziuba ^{1,2}, Theresa Zwiener,¹ Rene Uebe¹ and Dirk Schüler^{1*}

¹Department of Microbiology, University of Bayreuth, Bayreuth, Germany.

²Institute of Bioengineering, Research Center of Biotechnology of the Russian Academy of Sciences, Moscow, Russia.

Summary

The magnetotactic lifestyle represents one of the most complex traits found in many bacteria from aquatic environments and depends on magnetic organelles, the magnetosomes. Genetic transfer of magnetosome biosynthesis operons to a non-magnetotactic bacterium has only been reported once so far, but it is unclear whether this may also occur in other recipients. Besides magnetotactic species from freshwater, the genus *Magnetospirillum* of the *Alphaproteobacteria* also comprises a number of strains lacking magnetosomes, which are abundant in diverse microbial communities. Their close phylogenetic interrelationships raise the question whether the non-magnetotactic magnetospirilla may have the potential to (re)gain a magnetotactic lifestyle upon acquisition of magnetosome gene clusters. Here, we studied the transfer of magnetosome gene operons into several non-magnetotactic environmental magnetospirilla. Single-step transfer of a compact vector harbouring >30 major magnetosome genes from *M. gryphiswaldense* induced magnetosome biosynthesis in a *Magnetospirillum* strain from a constructed wetland. However, the resulting magnetic cellular alignment was insufficient for efficient magnetotaxis under conditions mimicking the weak geomagnetic field. Our work provides insights into possible evolutionary scenarios and potential limitations for the dissemination of magnetotaxis by horizontal gene transfer and

expands the range of foreign recipients that can be genetically magnetized.

Introduction

The genus *Magnetospirillum* of the *Alphaproteobacteria* was described in 1991 based on the first cultured magnetotactic bacteria (MTB) that had been isolated from freshwater sediments by taking advantage of their active, directed motility in magnetic fields (Schleifer *et al.*, 1991). The first species found to be affiliated with this genus by 16S rRNA sequence analysis were *Magnetospirillum magnetotacticum* MS-1 (formerly *Aquaspirillum magnetotacticum*) (Blakemore *et al.*, 1979; Frankel *et al.*, 1979; Maratea and Blakemore, 1981), *M. gryphiswaldense* MSR-1 (Schüler and Köhler, 1992) and *M. magneticum* AMB-1 (Matsunaga *et al.*, 1991). By exploiting their magnetotaxis, a number of further magnetotactic spiral bacteria were later isolated and identified as members of *Magnetospirillum* (Schüler *et al.*, 1999; Lefevre *et al.*, 2012; Wang *et al.*, 2015; Dziuba *et al.*, 2016; Ke *et al.*, 2018).

All magnetotactic magnetospirilla share a helical cell morphology, motility by means of a single flagellum at each pole and the ability of microoxic or anoxic denitrifying growth on short-chained fatty acids. Their magnetotactic behaviour is caused by the presence of dedicated magnetic organelles, termed magnetosomes, which consist of membrane-enveloped cuboctahedral magnetite (Fe₃O₄) crystals aligned in a single chain. The magnetosomes are thought to align MTB cells along vertically inclined geomagnetic magnetic field lines, which in conjunction with aerotactic sensing and active swimming facilitate their navigation along redox gradients towards suboxic layers within chemically stratified aquatic sediments (Popp *et al.*, 2014; Uebe and Schüler, 2016). To date, members of the genus *Magnetospirillum* represent the best-studied MTB in terms of physiology and magnetosome biosynthesis (Komeili, 2012; Uebe and Schüler, 2016). In *M. gryphiswaldense* MSR-1, magnetosome biomineralization was found to be strictly controlled by gene clusters comprising >30 genes that

Received 12 December, 2019; revised 3 February, 2020; accepted 18 February, 2020. *For correspondence. E-mail dirk.schueler@uni-bayreuth.de; Tel. +49 (0)921 552729.

are located within a chromosome region termed the genomic magnetosome island (MAI) (Schübbe *et al.*, 2003), which later was found to be conserved in all magnetic members of this genus (Matsunaga *et al.*, 2005; Koziava *et al.*, 2016, 2019; Smalley *et al.*, 2016). Whereas the presence of magnetosomes was initially proposed as a distinct feature of *Magnetospirillum* species, more recently a number of non-magnetic helical-shaped bacteria were isolated from various habitats, including freshwater sediments and wetlands, by selection for specific metabolic properties rather than by magnetic collection. Although the non-magnetic strains were affiliated to *Magnetospirillum* based on 16S rRNA phylogeny and shared the characteristic morphological and physiological features of the genus, they were unable to produce magnetosomes. Several non-magnetotactic *Magnetospirillum* spp. were isolated based on their ability to anaerobically degrade recalcitrant aromatic compounds that make them interesting for bioremediation applications (Shinoda *et al.*, 2000, 2005; Lahme *et al.*, 2014; Meyer-Cifuentes *et al.*, 2017b). For instance, a strain *Magnetospirillum* sp. 15-1 was isolated from a toluene-degrading consortium in a reconstructed wetland (Meyer-Cifuentes *et al.*, 2017b). Another strain, *M. bellicus* VDY, isolated from a bioelectrical reactor is distinguished by its ability of respiration using perchlorate (Thrash *et al.*, 2010). The non-magnetic strain *M. aberrantis* SpK was isolated in the attempt to obtain MTB by magnetic enrichment, however in fact it did not demonstrate magnetotaxis and contained only rare and irregular iron-containing inclusions, but no magnetosomes, suggesting that it was likely isolated due to its high motility and strong negative aerotaxis rather than magnetic response (Gorlenko *et al.*, 2011). In addition, many uncultivated *Magnetospirillum* spp. were identified in metagenomic libraries from freshwater sediments, soils and rhizosphere samples, indicating their high abundance and activity in a number of habitats (Lu *et al.*, 2006; Borole *et al.*, 2009; van der Lelie *et al.*, 2012; Lin *et al.*, 2013; Yin *et al.*, 2015; Bourceret *et al.*, 2018; Mediavilla *et al.*, 2019).

The absence of magnetosomes in the non-magnetotactic *Magnetospirillum* spp. is consistent with the lack of conserved magnetosome genes as revealed by genome sequencing for several of the isolates (Dzyuba *et al.*, 2012; Meyer-Cifuentes *et al.*, 2017a), (unpublished genome is also available for *M. bellicus* VDY from the Integrated Microbial Genomes and Microbiomes (IMG/M) under the link: https://img.jgi.doe.gov/cgi-bin/m/main.cgi?section=TaxonDetail&page=taxonDetail&taxon_oid=2546825520). However, non-magnetotactic *Magnetospirillum* spp. interlace with the magnetotactic species in the phylogenetic tree, rather than form a separate cluster (Fig. 1A). This suggests that several independent events of magnetosome gene losses may have happened within the genus in the evolutionary past, and indeed spontaneous

losses of magnetosome gene clusters have been frequently observed in MSR-1 and other magnetic magnetospirilla under stress conditions (Schübbe *et al.*, 2003; Fukuda *et al.*, 2006).

On the other hand, the recently reported evidence for the horizontal transfer (HGT) of magnetosome genes between different species of *Magnetospirillum* suggests a complex evolutionary history of magnetotaxis within the genus, which includes both losses and (re)gains of the magnetosome genes (Lefevre *et al.*, 2012). This raises the question of whether the non-magnetotactic magnetospirilla still retain the potential to switch to a magnetotactic lifestyle upon acquisition of magnetosome gene clusters that has not been experimentally addressed yet. Successful functional expression of major magnetosome gene operons has been limited so far to the only foreign organism, i.e. photosynthetic *Rhodospirillum rubrum* (Kolinko *et al.*, 2014), but remained an unsolved challenge in all other tested *Alphaproteobacteria*, possibly because of so far underestimated complexity of the process (Dziuba and Schüler, in preparation).

In this study, we addressed this question by attempting chromosomal integration of the major magnetosome operons from MSR-1 into three non-magnetotactic *Magnetospirillum* spp.: *M. bellicus* VDY, *M. aberrantis* SpK and *Magnetospirillum* sp. 15-1. To facilitate the gene transfer, we constructed a compact vector that enabled the single-step transfer of all magnetosome operons. While the transformation of VDY and SpK was prevented by the presence of a restriction–modification system(s), chromosomal insertion of the magnetosome gene cassette in *Magnetospirillum* sp. 15-1 induced the biosynthesis of magnetosomes causing a magnetic response. However, magnetite crystals produced by 15-1 were smaller and lacked the regular chain organization of the donor, probably due to unbalanced expression of several magnetosome proteins, and were insufficient for efficient magnetotaxis under conditions mimicking the weak geomagnetic field. Our work provides insights into possible evolutionary scenarios and potential limitations for the dissemination of magnetotaxis by horizontal gene transfer and will stimulate future studies on the functional reconstruction of magnetosome biosynthesis in other organisms. Given the ability of many non-magnetotactic magnetospirilla to degrade xenobiotics, our study also opens routes towards engineering of magnetically controllable organisms for bioremediation.

Materials and methods

Strains and cultivation condition

Bacterial strains are listed in Table 1. Unless specified otherwise, *Magnetospirillum gryphiswaldense*, *Magnetospirillum*

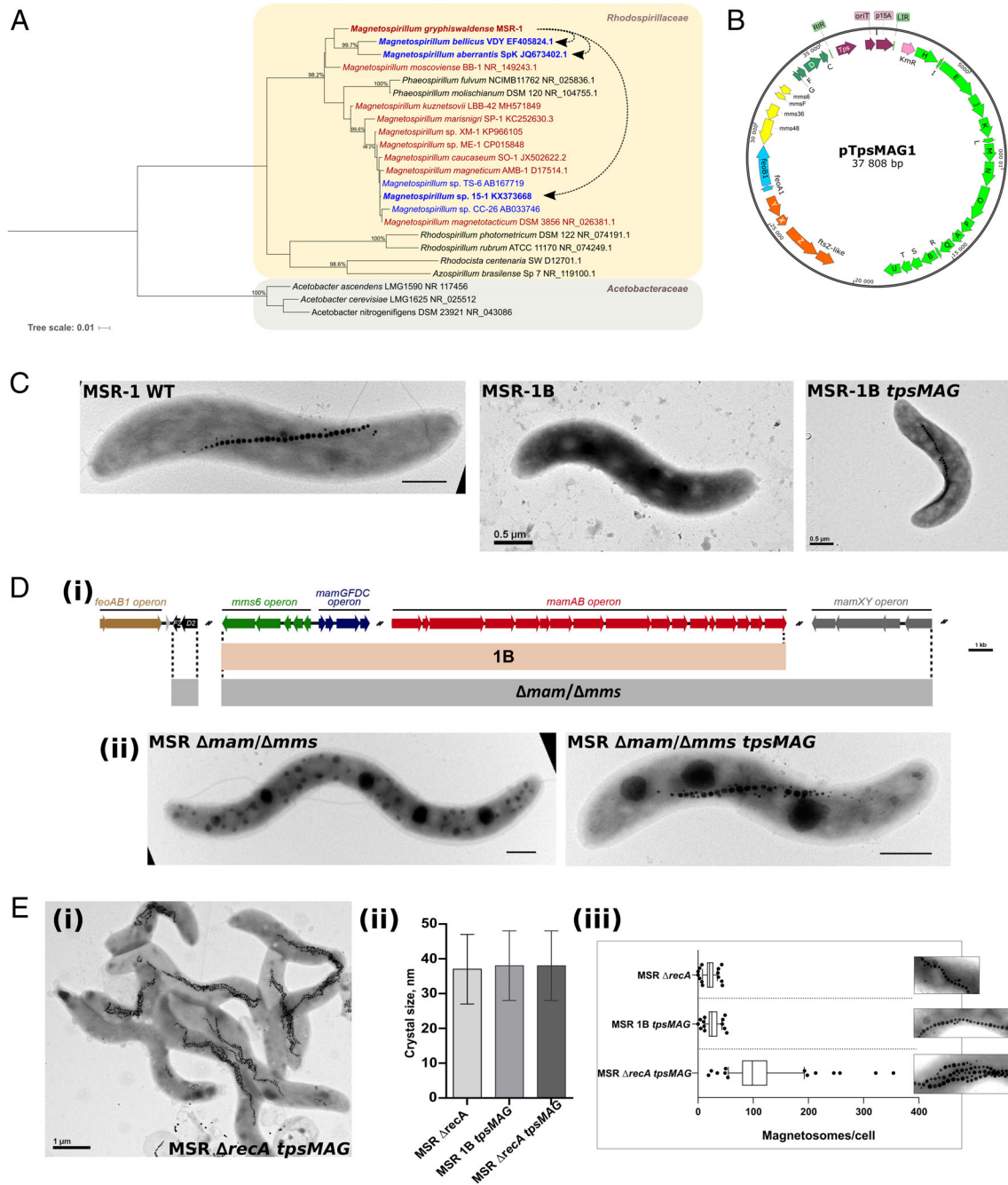


Fig. 1. (A) Maximum likelihood phylogenetic tree based on 16S rRNA demonstrating relationships within the genus *Magnetospirillum* spp. Magnetotactic strains marked in brown, non-magnetotactic—in blue. Strains used in this study are highlighted in bold. Arrows indicate the direction of magnetosome genes transfer in this study. B. Vector map of pTpsMAG1. In green—*mamAB* operon, orange—*mamYXZ*, blue—*feoAB1*, yellow—*mms6op*, dark green—*mamGFDC*. RIR and LIR, right and left inverted repeats; *oriT*, the origin of transfer; *p15a*, the origin of replication. The *mamAB* operon includes several genes that are essential for magnetosome formation, e.g. *mamB*, *mamM*, *mamE*, *mamO*, *mamQ*, *mamL* and *mamI*. The genes *mamK*, *mamJ* and *mamY* are responsible for magnetosome chain assembly and positioning. The *feoAB1* operon encodes an additional system for transport of ferrous iron, and the other genes encode accessory factors regulating size and shape of crystals. C. TEM micrographs of MSR wild type (MSR-1 WT), non-magnetic spontaneous mutant MSR-1B and the same mutant complemented with pTpsMAG1 (MSR-1B *tpsMAG*). D. Construction and complementation of MSR $\Delta\text{mam}/\Delta\text{mms}$ mutant: (i) regions deleted in the spontaneous non-magnetotactic mutant MSR-1B (beige baulks) and in MSR $\Delta\text{mam}/\Delta\text{mms}$ (grey baulks); (ii) TEM micrographs of MSR $\Delta\text{mam}/\Delta\text{mms}$ and the same mutant complemented with pTpsMAG1 (MSR $\Delta\text{mam}/\Delta\text{mms}$ *tpsMAG*). E. Reconstruction of the magnetosome overproducing MSR strain with pTpsMAG1: (i) TEM micrograph of the mutant, (ii) magnetosome size ($N_{\text{mag}} \geq 500$), and (iii) number ($N_{\text{cell}} \geq 100$) in MSR ΔrecA *tpsMAG* in comparison to the parental strain and MSR-1B *tpsMAG*.

Table 1. Bacterial strains used in the study.

Name	Genotype	Characteristics	Source/References
<i>Magnetospirillum gryphiswaldense</i> MSR-1	WT	Model magnetotactic organism, donor of magnetosome genes for the genetic construct	(Schleifer <i>et al.</i> , 1991), DSM-6361
<i>Magnetospirillum aberrantis</i> SpK	WT	Non-magnetotactic member of genus <i>Magnetospirillum</i>	(Gorlenko <i>et al.</i> , 2011), from the strain collection of Laboratory of molecular identification, FRC Fundamentals of Biotechnology RAS, Moscow, Russia
<i>Magnetospirillum bellicus</i> DSM21662	WT	Non-magnetotactic member of genus <i>Magnetospirillum</i>	DSMZ, (Thrash <i>et al.</i> , 2010)
<i>Magnetospirillum</i> sp. 15-1 'Meyer'	WT	Non-magnetotactic member of genus <i>Magnetospirillum</i>	(Meyer-Cifuentes, Martinez-Lavanchy, <i>et al.</i> , 2017), kindly provided by Dr. Heipieper and Dr. Meyer-Cifuentes (Helmholtz Centre for Environmental Research – UFZ), Leipzig, Germany
<i>E. coli</i> NEB10 β	F ⁻ <i>mcrA</i> Δ (<i>mrr-hsd-RMS-mcrBC</i>) Φ 80/ <i>lacZ</i> Δ M15 Δ <i>lacX74 endA1 recA1 deoR</i> Δ (<i>ara.leu</i>)7697 <i>araD139 galU galK nupG rpsL</i> λ ⁻	The strain was used for construction and cloning of pTpsMAG1	Purchased from NEB BioLabs (MA, USA)
<i>E. coli</i> WM3064	<i>thrB1004 pro thi rpsL hsdS lacZ</i> Δ M15 RP4-1360 Δ (<i>araBAD</i>) 567 Δ <i>dapA1341::[erm pir]</i>	Donor strain for transformation by conjugation, α,ϵ -diaminopimelic acid (DAP) auxotroph	William Metcalf, UIUC, unpublished

aberrantis, *Magnetospirillum bellicus* and *Magnetospirillum* sp. 15-1 were cultivated microaerobically in modified flask standard medium (FSM) at 30 °C and 120 rpm agitation (Heyen and Schüler, 2003). *Escherichia coli* strains were cultivated in lysogeny broth as described elsewhere (Sambrook and Russell, 2001). Cultures of *E. coli* WM3064 (W. Metcalf, unpublished) were supplemented with 0.1 mM of DL- α,ϵ -diaminopimelic acid and supplied with 25 μ g/ml of kanamycin when necessary. Selection for transconjugants was carried out on agar-solidified media (1.5% (w/v)), supplemented with 5 μ g/ml kanamycin. Optical densities were measured photometrically at 565 nm for *Magnetospirillum* spp. and 600 nm for *E. coli*. The coefficient of magnetically induced differential light scattering (Cmag) was measured as reported (Schüler *et al.*, 1995).

Molecular and genetic techniques

Plasmids used for this study are listed in Table 2, primers are listed in Table S1. The vector pTpsMAG1, comprising

the set of five major magnetosome operons from MSR-1, was constructed on the basis of plasmid pTpsABG6 (29.95 kb) that already contained *mamAB*, *mamGFDC* and *mms6* operons (Kolinko *et al.*, 2014). First, *mamXYZ* and *feoAB1* operons together with approximately 200–300 bp of upstream and downstream regions containing putative native regulatory elements were amplified by a high fidelity polymerase Q5 (New England Biolabs, New England USA) from the genomic DNA of MSR-1 using primers with NotI restriction sites and unique nucleotide sequences as overhangs for subsequent Gibson assembly (Torella *et al.*, 2014). The fragments were assembled into a pUC19 derivative cloning vector by Gibson reaction as described (Torella *et al.*, 2014) and cloned into *E. coli* DH5 α . The fragment containing both operons was excised from the vector by NotI and ligated into NotI-digested pTpsABG6 resulting in plasmid pTpsMAG1 (37.8 kb). Because of the p15a ori, pTpsMAG1 is unable to replicate in the target hosts but integrates its expression cassette randomly into a chromosome by MycoMar

Table 2. Plasmids used in the study.

Plasmid	Characteristics	Source/Reference
pSC101-BAD-gbaA	TcR, replicative plasmid containing <i>redα/redβ</i> recombinases under the control of a L-arabinose inducible promoter for recombineering	(Wang <i>et al.</i> , 2006)
pTpsABG6	CmR, KmR, p15A ori, mariner <i>tps mamAB, mamGFDC, mms6</i>	(Kolinko <i>et al.</i> , 2014)
pTpsMAG1	CmR, KmR, p15A ori, mariner <i>tps mamAB, mamGFDC, mms6, mamXYZ, feoAB1</i>	This study
pORdmms5-mmxF	pORFM-Galk derivative (Raschdorf <i>et al.</i> , 2014), <i>mms5</i> (<i>mamD2F2</i>) operon up- and down-stream regions for its <i>in-frame</i> deletion	This study
pTZ051	pORFM-Galk derivative (Raschdorf <i>et al.</i> , 2014), <i>mamXY</i> upstream and <i>mms6</i> downstream regions for its <i>in-frame</i> deletion	This study

mariner transposase (*tps*). Cloning of pTpsMAG1 was conducted in *E. coli* NEB10 β due to its improved ability to stably maintain large vectors.

Construction of MSR-1 Δ *mam*/ Δ *mms* mutant

To analyse the restoration of a magnetic phenotype in MSR-1 as the positive control, a non-magnetic, unmarked *mam/mms* null mutant was generated using RecA-mediated homologous recombination (Raschdorf *et al.*, 2014). Therefore, 1–1.5 kb up- and down-stream regions of the *mms5*, *mms6* and *mamXY* operons were amplified, fused by an overlapping PCR and ligated into an EcoRV digested pORFM-GalK vector. The plasmids were successively transferred into the Δ A13 mutant, which already lacked *mamAB* and *mamGFDC* operons (Lohße *et al.*, 2011), by conjugation using *E. coli* WM3064 as a donor strain. Insertion mutants were selected using kanamycin agar plates and scaled up to 1 ml. After counter-selection with galactose, correct Δ *mam*/ Δ *mms* deletions were verified by PCR.

Screening of transconjugants and PCR-test for the cassette integrity

All plasmids were transferred into the target hosts by biparental conjugation using *E. coli* WM3064 as donor strain, generally according to the procedure described in Schultheiss and Schöler (2003). After conjugation, kanamycin-resistant transconjugants were transferred into 96-well plates filled with 200- μ l of the corresponding medium containing the appropriate kanamycin concentration. Transconjugants were then screened for the integration of the magnetosome expression cassette using primers that bind within *mamY* and *feoA* respectively (primers 5 and 6 in Table S1). Subsequently, PCR tests for the integrity of the transferred operons in the mutants were conducted using primers designed in a way that the resulting PCR fragments cover most of the transferred cassette (primers 5–22 in Table S1).

Transmission electron microscopy

For transmission electron microscopy (TEM) analyses, the strains were cultivated under microoxic conditions in FSM to enable potential magnetosome formation. Cells were harvested from overnight cultures by centrifugation, adsorbed onto carbon-coated copper-mesh grids and washed two times with water. Samples were imaged with a JEOL 1400 TEM (Japan) at 80 kV acceleration. Micrographs were analysed with tools implemented in the ImageJ software (Abràmoff *et al.*, 2004).

Analysis of cell response to external magnetic field

Magnetic response of cells was analysed by semisolid swarm agar plate assays or microscopic observations employing adjustable external magnetic fields. For swarm agar assays, 5 μ l of overnight cultures diluted to OD 0.1 were stabbed into semisolid 0.3% FSM agar and incubated at 28 °C for 1–7 days in the horizontal magnetic field (600 μ T) generated by a pair of coils.

Swimming behaviour of cells in external magnetic field was also observed and recorded using dark-field microscopy under an upright FN1 Eclipse (Nikon) microscope at 20 \times magnification. To this end, 3 μ l cell suspensions were placed under a coverslip and sealed with wax. Homogeneous magnetic fields of 400 μ T were applied using a custom-manufactured (Claricent, Munich, Germany) magnetic coil cage ('magnetodrom', (Popp *et al.*, 2014)) consisting of three pairs of coils positioned along X-, Y- and Z-axes. To observe the switch of cells swimming direction, the magnetic field direction was altered between X- and Y-axes at a frequency of 0.1 s⁻¹. Videos were recorded with a pco.edge 4.2 sCMOS camera at a frame rate of 25 fps controlled by NIS-Elements 5.1 software (Nikon).

Magnetosome isolation

Cells were cultivated in 8 l of FSM medium in screw-cap bottles for 1–2 days. All steps of isolation were performed at 4 °C. Cells were harvested by centrifugation at 4000 rpm (Sorvall RC5B Plus, Thermo Scientific), re-suspended in 30 ml of re-suspension buffer [50 mM Hepes, 1 mM EDTA, 0.1 mM phenylmethylsulfonyl fluoride (PMSF)], homogenized and lysed by several passages through a Microfluidizer Laboratory Homogenizer (Microfluidics Corp., MA, USA). Cell lysates were centrifuged for 10 min at 1000 rpm to remove cell debris. Magnetosomes were separated in 5 ml MACS columns (Miltenyi Biotec) placed between neodymium-iron-boron cube magnets (gravity flow), essentially as described in Raschdorf and colleagues (2018b). The magnetically enriched magnetosome fraction was additionally purified and concentrated by ultracentrifugation at 100 000g with a 60% sucrose cushion (Sorvall WX Ultra 80, Thermo Scientific).

SDS-PAGE and western blot

Bacterial cells for SDS-PAGE were concentrated to optical density of 10, whereas magnetosome samples were normalized to OD₄₀₀ of 0.025 per loading, mixed with sample buffer (58 mM Tris-HCl pH 6.8, 2% SDS, 5% glycerol, 0.1 M DTT, 0.01% bromophenol blue) and heated at 99 °C for 10 min. Proteins were resolved in

12%–22.5% SDS-PAGE gels (0.5 mA cm⁻²) using Tris-glycine running buffer (50 mM Tris-HCl pH 8.5, 0.19 M glycine, 0.1% SDS) as described (Fling and Gregerson, 1986). For stain-free imaging of proteins, 2,2,2-trichloroethanol was added to all gels at a final concentration of 0.5% (w/v). Proteins were detected in gels and on blotted membranes by the stain-free technique according to the method described by Ladner and colleagues (2004). Separated proteins were blotted onto 0.22 or 0.45 µm PVDF membranes by the semi-dry technique at 2 mA cm⁻² for 2 h, with Bjerrum-Schafer-Nielsen transfer buffer (48 mM Tris-base, 39 mM glycine, 0.0375% SDS, 20% methanol) (Bjerrum and Schafer-Nielsen, 1986). After transfer, membranes were blocked in 5% non-fat milk in TBS (50 mM Tris-HCl pH 7.5, 150 mM NaCl) for 1 h and subsequently incubated with primary antibodies overnight. Custom rabbit polyclonal primary antibodies used in this study were purchased from companies Pineda Antikörper-Service (Germany) and ProteoGenix (France). Membranes were washed four times with TTBS (buffer) (0.05% Tween 20, 50 mM Tris-HCl pH 7.5, 150 mM NaCl) and incubated with HRP-labelled anti-rabbit secondary antibodies for 1 h, followed by subsequent washing with TTBS. Immunodetection was performed by a chemiluminescent technique using the commercial Western BLoT Chemiluminescence HRP Substrate by Takara Bio (USA). Gel and blot documentation was performed using ChemiDoc™ XRS+ System (Bio-Rad, USA), and the images were processed with ImageLab 6.0.1 software.

Bacterial cell extract preparation

Cells were grown in 100 ml of FSM at 30 °C ON, harvested by centrifugation (4500 rpm, 4 °C, 10 min). The pellets were washed by sterile PBS (137 mM NaCl, 2.7 mM KCl, 10 mM Na₂HPO₄, 1.8 mM KH₂PO₄, pH 7.2) supplied with 0.1 mM PMSF and re-suspended in 5 ml of the same buffer, which was additionally supplied with 0.25 mg/ml of lysozyme and 5 mM EDTA. The cells were lysed by 3 cycles of freezing at -80 °C and thawing. The cell debris was centrifuged at 5000g (4 °C, 10 min) and cell extracts in the supernatant were collected. The cell extracts were used immediately or supplied with 10% glycerol and stored at -80 °C.

Treatment of plasmid DNA with bacterial cell extract

For the DNA digestion experiments the cell extracts were mixed with 1× Tango buffer (33 mM Tris-acetate, pH 7.9, 10 mM magnesium acetate, 66 mM potassium acetate, 0.1 mg/ml BSA, Thermo Fisher Scientific) and 0.5–1 µg plasmid DNA isolated from *E. coli* strain NEB10β or MSR-1 in total volume of 20 µl. The reactions were incubated at 37 °C for 30 min. As a control, plasmid DNA

was incubated with water, without cell extract. The resulting fragments were visualized by 1% agarose electrophoresis.

Phylogenetic inference and bioinformatics methods

The maximum-likelihood phylogenetic tree based on the partial sequences of 16S rRNA genes (1314 bp) was reconstructed using IQ-Tree under TIM2 + I + G model suggested by ModelFinder (Nguyen *et al.*, 2015; Kalyaanamoorthy *et al.*, 2017). Sequences for the phylogenetic analysis were taken from GeneBank. The phylogenetic trees were visualized and annotated by iTOL online tool (Letunic and Bork, 2019). All sequences we edited and analysed using Geneious 8.1.4 (<https://www.geneious.com/>).

Statistical methods

Plotting of graphs and basic statistical analysis was implemented in GraphPad Software (v. 6.01 for Windows). The statistical significance of the differences in magnetosome size and number were evaluated by one-way analysis of variance and Kruskal-Wallis test followed by unpaired *t*-test with Welch's correction and Mann-Whitney *U* test, with the *p*-value threshold of 0.05.

Images processing

The raster images were processed in PaintNET software (v. 4.2), the figures were prepared using scalable vector graphic (SVG) software Inkscape 0.92 (<https://inkscape.org>). The vector map was prepared using SnapGene software (GSL Biotech; available at snapgene.com).

Results

A single compact vector comprising the major magnetosome biosynthesis gene clusters restores magnetosome formation in MSR Δmam/Δmms and causes magnetosome overproduction in MSR ΔrecA

To simplify the transfer of magnetosome genes into the target hosts, a single vector harbouring the five most important operons for magnetosome formation in MSR-1, *mamAB*, *mamGFDC*, *mamYXZ*, *mms6* and *feoAB1*, including their native promoters, was constructed. This was achieved by incorporation of *mamYXZ* and *feoAB1* into plasmid pTpsABG6, which already harboured the other three operons (Kolinko *et al.*, 2014). The resulting vector, designated pTpsMAG1 (refers to magnetosome biosynthesis), shares the basic features intrinsic to the parental vector, e.g. p15a origin, mariner transposase *tps*

for chromosomal insertion and the gene for kanamycin resistance (Fig. 1B).

In order to test pTpsMAG1 for the ability to functionally reconstitute magnetosome formation, it was first conjugated into the spontaneous non-magnetotactic mutant of MSR-1, termed MSR-1B (Schübbe *et al.*, 2003). The resulting mutants formed wild type-like (WT-like) magnetosomes, as expected (Fig. 1C). However, it was important to further include into transformation experiments as positive control a strain, in which magnetosome formation can be easily monitored and the magnetic phenotype is immediately evident by biomass colour or cell magnetic response since spontaneous mutations of magnetosome biosynthesis genes were occasionally observed in the vector during propagation in the donor *E. coli* strain (data not shown). However, since MSR-1B still possesses the *mamYXZ* operon (Schübbe *et al.*, 2003), it could not serve as 'clean' positive control. Therefore, we set out to construct a $\Delta mam/\Delta mms$ mutant of MSR-1. This was achieved by allelic replacement resulting in the mutant lacking all *mam* and *mms* operons including their interspersing regions with ~66 kb extent of deletion (Fig. 1D-i). As expected, the mutant was non-magnetic and entirely devoid of magnetosomes. As in MSR-1B, complementation with pTpsMAG1 virtually restored a WT-like magnetosome phenotype in MSR-1 $\Delta mam/\Delta mms$ (Fig. 1D-ii). Next, we transferred pTpsMAG1 into MSR-1 $\Delta recA$, a strain forming WT-like magnetosomes that resulted in strains having two copies of all five operons in its chromosome (Kolinko *et al.*, 2011). As expected, the resulting mutant was able to produce multiple magnetosome chains with >100 magnetosomes per cell, similar to the phenotype reported previously (Lohße *et al.*, 2016) (Fig. 1E).

Genetic transfer of pTpsMAG1 into M. aberrantis and M. bellicus is prevented by a putative restriction–modification barrier

Next, we attempted to transfer pTpsMAG1 vector into three naturally non-magnetotactic *Magnetospirillum* strains by conjugation. However, despite repeated attempts to transform *M. aberrantis* and *M. bellicus*, no transconjugant colonies for these two species could be obtained, independent of variations in growth conditions. Therefore, we hypothesized that some kind of restriction–modification system might prevent transformation in case of these two *Magnetospirillum* species. Indeed, treatment of plasmid DNA isolated from *E. coli* WM3064 (pTpsMAG1) or a broad-host vector plasmid isolated from MSR-1 (pBBR-MCS2) with cell extracts from the strains sheared it into smearing fragments within 30 min of incubation at 37 °C (Fig. 2). In contrast, cell extracts prepared from MSR-1, a strain that can be transformed with high rates, and

Magnetospirillum sp. 15-1 did not digest DNA under the same conditions. This suggested that *M. bellicus* and *M. aberrantis* may employ one or several efficient restriction-modification (RM) system(s) for self-protection from the invading foreign DNA that is known to hamper genetic manipulation of some non-model bacterial species (Donahue *et al.*, 2000). Therefore, further attempts to transform *M. aberrantis* and *M. bellicus* were abandoned in the current study.

Transfer of pTpsMAG1 into Magnetospirillum sp. 15-1 induces magnetosome formation in the strain

In contrast to *M. aberrantis* and *M. bellicus*, after 10 days of incubation under microoxic conditions (2% O₂, 98% N₂), a few colonies of transconjugants appeared on agar plates in case of *Magnetospirillum* sp. 15-1. Three out of five clones, in which the integrity of the magnetosome gene expression cassette was confirmed by PCR (Fig. S1), were selected for further analysis (clones C5, C7 and C9). Remarkably, the cell pellets of the *Magnetospirillum* sp. 15-1 *tpsMAG1* mutants exhibited dark brown colour, in contrast to the beige colour of the WT (Fig. 3A). However, the difference in colour between WT and *tpsMAG1* mutants was less prominent in *Magnetospirillum* sp. 15-1 than in the complemented MSR-1 $\Delta mam/\Delta mms$ strain, which cell pellets had a clearly blackish colour (Fig. 3A). Consistently, the cultures of *Magnetospirillum* sp. 15-1 *tpsMAG1* demonstrated magnetic alignment measured by means of the light scattering method, with Cmag values of 0.5 ± 0.15 versus 1.3 ± 0.3 in MSR-1 (Fig. 3B) (Schüler *et al.*, 1995). Indeed, TEM analysis revealed the presence of electron-dense particles within the cells that confirmed the successful functional expression of the transferred genes (Fig. 3C). However, the 'magnetized' *Magnetospirillum* sp. 15-1 *tpsMAG1* mutants did not fully phenocopy the donor of magnetosome genes MSR-1. Instead, they synthesized magnetic particles that were not arranged in straight long chains, as in MSR-1, but were agglomerated, scattered, or occasionally formed short chains within the cells (Fig. 3C). Furthermore, the magnetosomes produced in *Magnetospirillum* sp. 15-1 *tpsMAG1* were significantly smaller than in the donor strain or the complemented $\Delta mam/\Delta mms$ *tpsMAG1* mutant, having magnetite crystal diameters of 21.5 ± 7.4 , 23.2 ± 7.1 and 23.9 ± 8.1 nm as measured in clones C5, C7 and C9 versus 34.5 ± 10.1 and 34.2 ± 9.6 nm in MSR-1 $\Delta mam/\Delta mms$ *tpsMAG1* clones (Fig. 3D).

All three tested clones of *Magnetospirillum* sp. 15-1 *tpsMAG1* demonstrated impaired growth in comparison to the WT (Fig. 4Ai-ii). They could reach approximately two-fold lower optical density in comparison to the wild type of *Magnetospirillum* sp. 15-1, whereas complementation

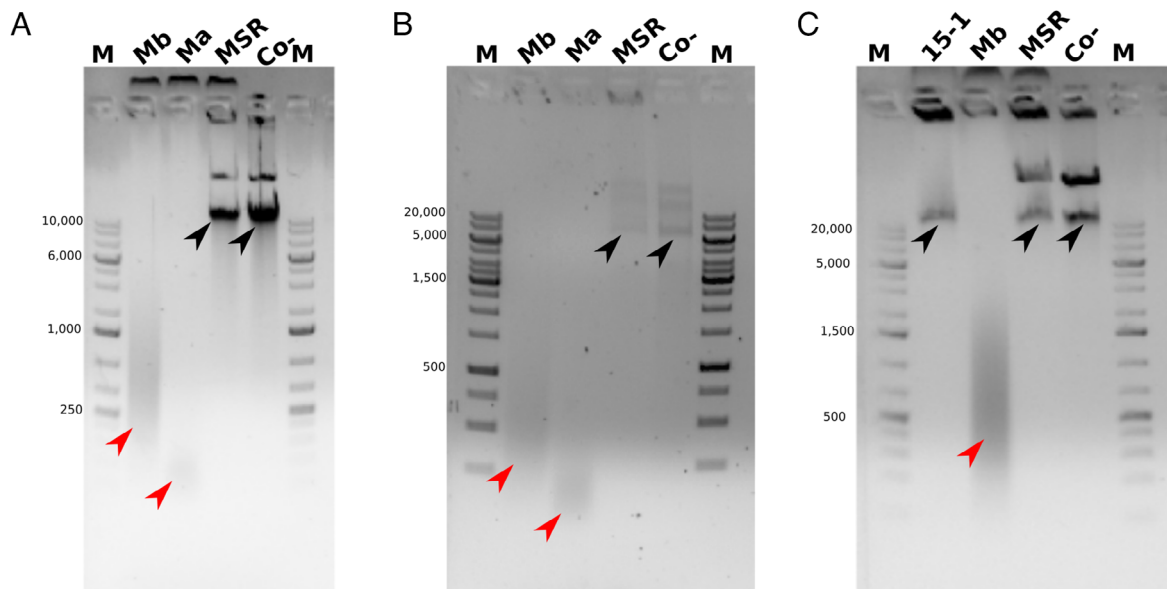


Fig. 2. Detection of putative restriction endonuclease activity in the cell extracts of *M. bellicus* and *M. aberrantis*. pTpsMAG isolated from *E. coli* (A, C) and a broad-host range vector pBBR-MCS2 isolated from MSR (B) were treated by cell extracts prepared from different strains: *M. bellicus* ('Mb'), *M. aberrantis* ('Ma'), *M. gryphiswaldense* ('MSR') and *Magnetospirillum* sp. 15-1 ('15-1') in 1× Tango buffer at 37 °C for 30 min. M, marker; Co- cell extract was replaced with water. Note the digestion of the plasmids treated by the cell extracts from *M. bellicus* and *M. aberrantis* (red arrowheads); the plasmids were not digested by cell extracts from MSR and *Magnetospirillum* sp. 15-1 (black arrowheads).

of MSR $\Delta mam/\Delta mms$ with pTpsMAG1 did not change the growth curves significantly in comparison to the parental strain MSR $\Delta mam/\Delta mms$. The decrease of fitness in the *Magnetospirillum* sp. 15-1 *tpsMAG* mutants was also indicated by a remarkable increase of doubling time, which varied among the clones ranging from 5.2 to 10.5 h versus ~3.6 h in the wild type (Fig. 4A-iii). In contrast, the growth rate in MSR $\Delta mam/\Delta mms$ *tpsMAG* remained mostly unaffected in comparison to the parental strain. This suggested that expression of magnetosome genes and/or magnetosome biosynthesis may impose a higher metabolic burden on *Magnetospirillum* sp. 15-1 than on the native host.

It has been well established that in the donor MSR-1 magnetosome production is stimulated by denitrifying conditions with nitrate as terminal electron acceptor (Heyen and Schüler, 2003). In the Δnap (lacking the periplasmic nitrate reductase) and $\Delta nirS$ (lacking the cytochrome *cd1* nitrite reductase) deletion strains of MSR-1 the magnetosome formation was severely impaired (Li *et al.*, 2012, 2013). *Magnetospirillum* sp. 15-1 was also capable of growth under anaerobic conditions with nitrate as a sole terminal electron acceptor (Fig. S2). However, in contrast to MSR-1, magnetosome production in *Magnetospirillum* sp. 15-1 *tpsMAG* mutants was not stimulated by dissimilatory nitrate reduction. On the contrary, the average magnetosome diameter in *Magnetospirillum* sp. 15-1 *tpsMAG* even slightly decreased with elevated nitrate

concentrations, which was also accompanied by decreased C_{mag} (Fig. S2). This result suggests that magnetosome biomineralization in *Magnetospirillum* sp. 15-1 *tpsMAG* is either not interlinked with nitrate respiration of the host, or their link is less efficient than in MSR-1.

Deficient magnetosome formation in Magnetospirillum sp. 15-1 tpsMAG is insufficient for effective magnetotaxis in Earth-range magnetic fields

Although the detectable C_{mag} indicated the ability of the *Magnetospirillum* sp. 15-1 *tpsMAG* to align in magnetic fields, the magnets commonly used for C_{mag} detection generate an artificially strong magnetic field of approximately 100 mT. Therefore, we studied whether magnetosomes formed in *Magnetospirillum* sp. 15-1 *tpsMAG* are sufficient to enable magnetotaxis in magnetic fields close to the strength of ambient geomagnetic fields (μT range). To this end, we subjected the mutants to swarm agar assays with constant magnetic field of 600 μT . In contrast to MSR-1, which formed swarming halos after 1–2 days after inoculation, the appearance of visible halos for *Magnetospirillum* sp. 15-1 required 7–8 days. However, unlike in MSR-1, *Magnetospirillum* sp. 15-1 *tpsMAG* swarming halos did not become distorted in the magnetic field direction but retained their spherical appearance (Fig. 4B). In consistence to this, no change

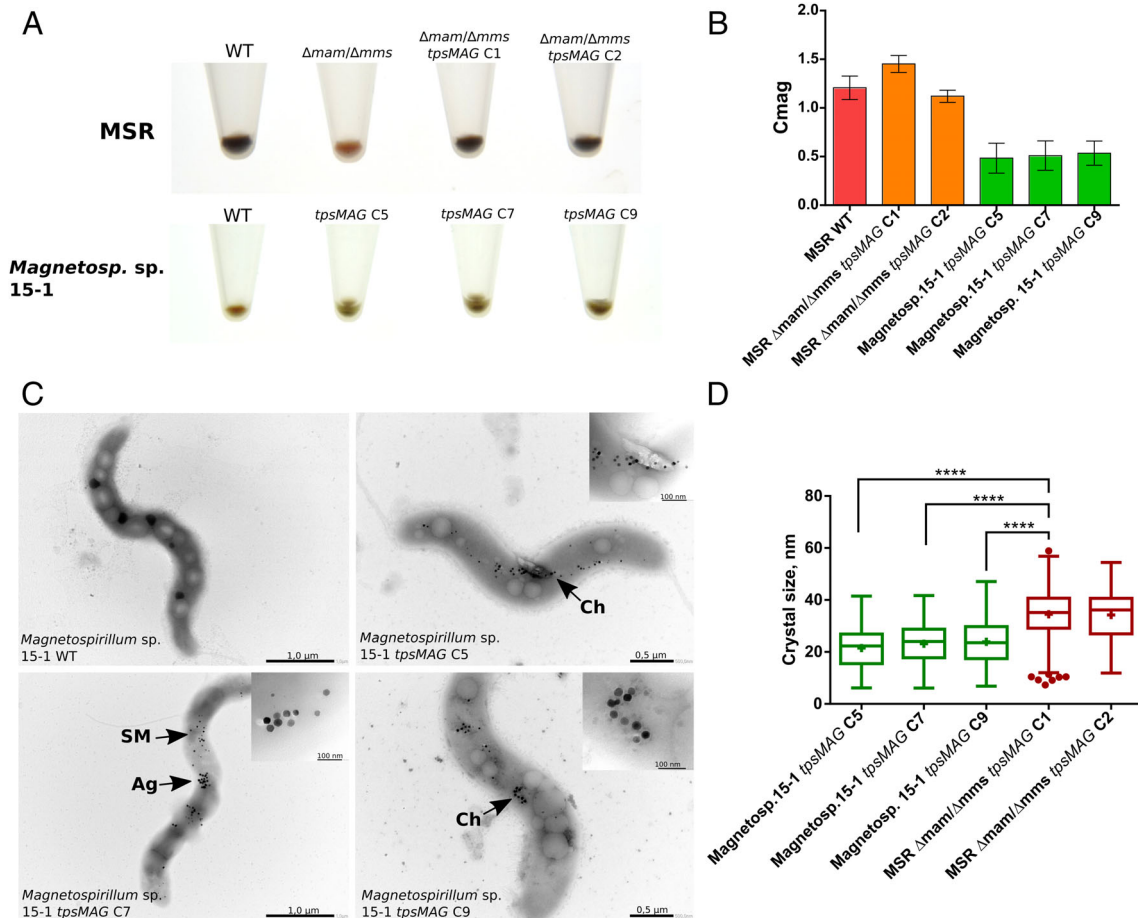


Fig. 3. Heterologous magnetosome biosynthesis by *Magnetospirillum* sp. 15-1. **A.** Biomass of the mutants of MSR-1 and *Magnetospirillum* sp. 15-1 in comparison to wild types (WT). **B.** Magnetic response of the cells measured by Cmag. Error bars represent standard deviations of the measurements made in three replicates, in three independent experiments. **C.** TEM micrographs of *Magnetospirillum* sp. 15-1 WT and *tpsMAG* mutants, exemplary cells and magnified magnetosomes. The heterogeneity of magnetosome organization within the cells is highlighted as the following: scattered (SM), agglomerated (Ag) and chain-like (Ch). **D.** Comparison of magnetosome crystal sizes between pTpsMAG1 transformed MSR and *Magnetospirillum* sp. 15-1 mutants. The asterisks represent points of significance (Mann–Whitney test).

in cell orientation and swimming behaviour could be observed during microscopic real-time recordings in the presence of alternating magnetic fields of 400 μ T (Movies S1–6). Taken together, this indicates that the magnetic moments of magnetosomes synthesized in *Magnetospirillum* sp. 15-1 *tpsMAG* did not endow the cells with effective magnetotaxis, at least in magnetic fields with the strengths ~8–12 times of the geomagnetic field.

Western blot analysis reveals differences in expression levels of magnetosome proteins MamB, MamY and Mms6 between Magnetospirillum sp. 15-1 tpsMAG and MSR-1

We reasoned that deficient chain organization and small magnetosome sizes in *Magnetospirillum* sp. 15-1 *tpsMAG* might be caused by imbalanced expression of one or more magnetosome proteins. Therefore, we

assessed the patterns of magnetosome proteins in the magnetosome membrane (MM) from the ‘magnetized’ mutants of *Magnetospirillum* sp. 15-1 by Western blot. First, we analysed intact magnetosomes isolated from the *Magnetospirillum* sp. 15-1 *tpsMAG* mutants for the expression of 11 magnetosome proteins encoded in the transferred cassette: MamJ, MamK, MamM, MamO, MamP, MamA, MamB, MamC, Mms6, MmsF and MamY (Fig. 5). The 1D SDS-PAGE proteins profile visualized by a stain-free method revealed many protein bands of the same molecular weight in the magnetosomes isolated from MSR-1 WT, MSR-1 Δ mam/ Δ mms *tpsMAG* and *Magnetospirillum* sp. 15-1 *tpsMAG* (Fig. 5A). However, there were also differences in the patterns and relative intensities of the bands. This fact can be partly attributed to the inevitable presence of contaminating cytoplasmic membrane proteins in the purified magnetosome samples (Raschdorf *et al.*, 2018a), which might differ

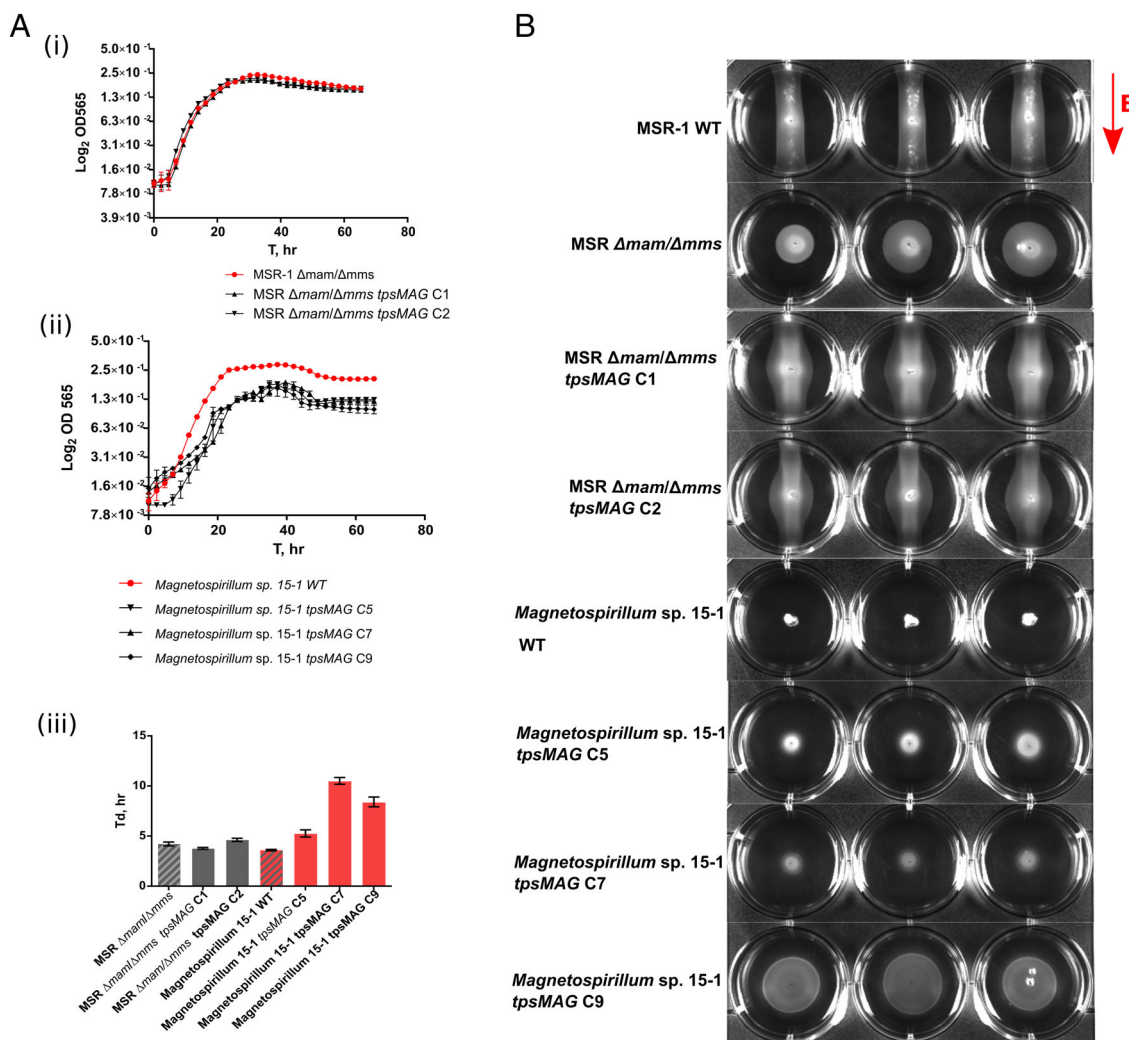


Fig. 4. (A) Growth tpsMAG mutants of: (i) MSR and (ii) *Magnetospirillum* sp. 15-1; (iii) doubling time of the mutants, MSR in grey, *Magnetospirillum* sp. 15-1 in red. Parental strains are highlighted with pattern. B. Swarm agar assay of the cultures in magnetic field ($600 \mu\text{T}$). Each well represents a biological replicate. B with arrow indicates the vector of the magnetic field lines. The results were reproduced in three independent experiments performed on different days.

in the two species and between preparations. On the other hand, this might also hint towards potential variations in gene expression levels between MSR-1 and *Magnetospirillum* sp. 15-1.

Among the tested proteins, MamJ and MamK were of particular interest with respect to the irregular magnetosome organization observed in *Magnetospirillum* sp. 15-1, as they represent the well-established key players of magnetosome chain assembly (Scheffel and Schüler, 2007; Katzmann *et al.*, 2010). The analysis showed that the band intensities of MamJ, detected in magnetosome samples of *Magnetospirillum* sp. 15-1, were similar to those in MSR-1 WT (Fig. 5B). Curiously, MamJ could not be detected in MSR-1 $\Delta\text{mam}/\Delta\text{mms}$ tpsMAG , although the observed WT-like magnetosome chain formation in

the mutant argues for the expression of the protein in the cells (Fig. 5B). In addition, MamK could be detected only in magnetosomes of MSR-1 WT, but not in MSR-1 $\Delta\text{mam}/\Delta\text{mms}$ tpsMAG and *Magnetospirillum* sp. 15-1 tpsMAG mutants, despite the regular magnetosome chains in MSR-1 $\Delta\text{mam}/\Delta\text{mms}$ tpsMAG . Although both MamJ and MamK are known to be associated with magnetosomes, they lack trans-membrane helices and are not *bona fide* MM proteins (Raschdorf *et al.*, 2018a), hence their virtual abundance in the magnetosome samples could be preparation-dependent. Therefore, we also estimated the abundance of these proteins in the crude cell extracts of *Magnetospirillum* sp. 15-1 tpsMAG mutants by Western blotting. The result revealed similar expression levels of MamJ and MamK in

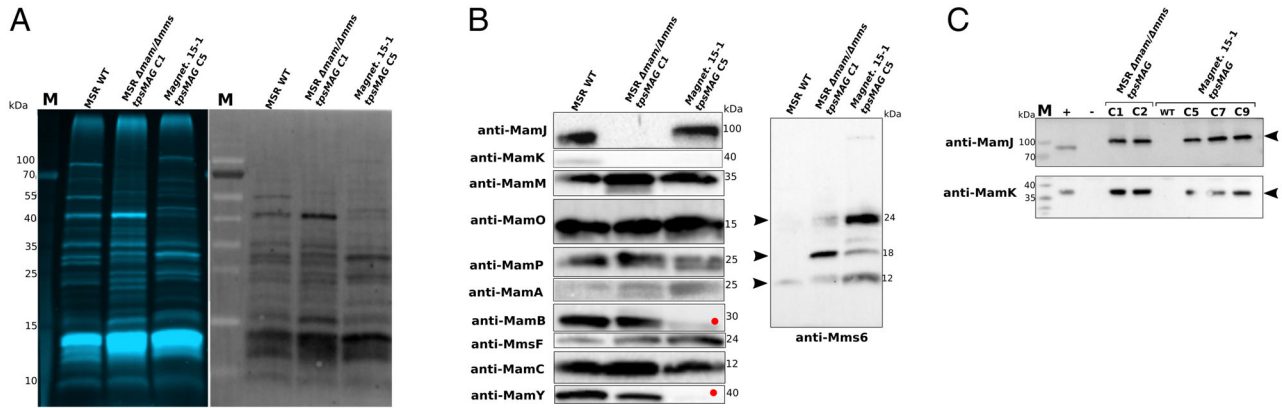


Fig. 5. Analysis of the magnetosome protein production in *Magnetospirillum* sp. 15-1 *tpsMAG* by Western blot. A. Protein profiles of the magnetosomes imaged by stain-free technique in 1D SDS-PAGE (left) and after transfer to the blot membrane (right). B. Western blot detection of magnetosome proteins in magnetosomes isolated from MSR-1 WT, MSR $\Delta mam/\Delta mms$ *tpsMAG* C1 and *Magnetospirillum* sp. 15-1 *tpsMAG* C5. C. Western blot detection of MamJ and MamK in whole-cell lysates of MSR WT, MSR $\Delta mam/\Delta mms$ *tpsMAG* C1 and *Magnetospirillum* sp. 15-1 *tpsMAG* C5. Red circles indicate the weak bands for MamB and MamY.

Magnetospirillum sp. 15-1 *tpsMAG* compared to both MSR-1 WT and MSR-1 $\Delta mam/\Delta mms$ (Fig. 5C), implying that MamK and MamJ were produced at sufficient levels.

Among the other proteins tested in the magnetosome samples, the signals detected for MamM, MmsF, MamC, MamA and MamP had similar intensities in *Magnetospirillum* sp. 15-1, MSR-1 WT and MSR-1 $\Delta mam/\Delta mms$ *tpsMAG*. The signals of MamB and MamY, however, appeared to be significantly weaker in *Magnetospirillum* sp. 15-1 in comparison to both MSR-1 WT and the complemented MSR-1 $\Delta mam/\Delta mms$ mutant (Fig. 5B). At the same time, Mms6, which usually appears as three bands presumably corresponding to dimers (~12 kDa), trimers (~18 kDa) and tetramers (~24 kDa) of the processed peptide (6 kDa), appeared to be more abundant in the magnetosomes from *Magnetospirillum* sp. 15-1 *tpsMAG* than in those from MSR-1 WT and MSR-1 $\Delta mam/\Delta mms$ *tpsMAG*. Intriguingly, in *Magnetospirillum* sp. 15-1 two additional bands, ~20 and ~100 kDa, were detected with anti-Mms6 antibodies, where the former might represent a product of degradation of a larger oligomer and the latter might correspond to a multiprotein complex, which includes Mms6. Taken together, the results of Western blot hint towards imbalanced expression of several magnetosome proteins in *Magnetospirillum* sp. 15-1 *tpsMAG* that could contribute to the observed magnetosome formation phenotype in the mutant.

Discussion

In the current study, we assessed the potential of three non-magnetotactic members of the genus *Magnetospirillum* to synthesize magnetosomes upon transfer of the key

magnetosome operons from MSR-1. Up to now, successful functional reconstruction of magnetosome biosynthesis has been achieved only in a single foreign organism, namely *R. rubrum*, while it failed so far in all other tested *Alphaproteobacteria* (Kolinko *et al.*, 2014; Dziuba and Schüler, in preparation). This suggests that some other factors outside the major biosynthetic operons might be important for successful biomineralization by a new host. In *R. rubrum* magnetosome operons were transferred in several sequential steps. In this study, to facilitate the transfer, we combined the five key magnetosome operons into a single vector (pTpsMAG1). The resulting plasmid can be applied in future studies to screen other foreign hosts applicable for magnetosome production in one-step transfer experiments. Transformation with pTpsMAG1 successfully endowed a non-magnetotactic strain *Magnetospirillum* sp. 15-1 with the ability for magnetosome biomineralization, thereby expanding the current set of foreign hosts for heterologous magnetosome biosynthesis. This also suggests that in addition to the ability of the host's transcription machinery to recognize the regulatory elements of the donor, the strain is likely to possess some yet unknown auxiliary genes in the genome that are essential for magnetosome biomineralization.

How non-magnetotactic species evolved within genus *Magnetospirillum* is still not clear. Several scenarios were proposed to explain the absence of magnetotaxis in these strains (Lefevre *et al.*, 2012). First, since cases of spontaneous loss of magnetosome genes and occurrence of non-magnetotactic phenotypes have been described in magnetospirilla MSR-1 and AMB-1 during cultivation in laboratory, deletion of magnetosome genes due to the inappropriate conditions upon isolation of the non-magnetotactic species cannot be excluded.

However, genetic analysis of spontaneous mutants of MSR-1 rather revealed diverse, mosaic-like deletion patterns, whereas simultaneous excision of all magnetosome genes at once has never been observed in MSR-1 (Schübbe *et al.*, 2003). Even in AMB-1, where a large 98 kb deletion spanning almost the entire MAI occurred systematically, several genes belonging to a smaller magnetosome 'islet' were not affected by the mutation (Fukuda *et al.*, 2006; Rioux *et al.*, 2010). In contrast, no remnants of MAI were found in the genomes of VDY, SpK and 15-1, and therefore it appears less likely that they lost the magnetotactic trait by a single deletion event due to the stress caused by laboratory cultivation. Considering this, a second scenario is highly plausible, which implicates that the spread of magnetosome genes in *Magnetospirillum* occurred by vertical transfer from a common magnetotactic ancestor followed by losses of the genes in particular groups within the genus. On the other hand, in addition to vertical inheritance, evidence for the recent horizontal transfer (HGT) of magnetosome genes between species within genus *Magnetospirillum* has been described in at least one case (Lefevre *et al.*, 2012). Taken together, this suggests a complex evolutionary history of magnetotaxis genes among *Magnetospirillum* spp. that includes a common magnetotactic ancestor, potential losses of the ability for magnetosome biosynthesis in several groups and occasional recent HGT of magnetosome genes between species. Our study demonstrates that non-magnetotactic members of genus *Magnetospirillum* can potentially acquire at least rudimentary ability for magnetosome biomineralization, which may similarly occur in the natural environment by HGT.

However, despite its close phylogenetic relationship to MSR-1, magnetosomes formed by *Magnetospirillum* sp. 15-1 appeared to be significantly smaller and less regularly organized within the cells. Swarm agar assay and growth-independent observations under the microscope in the presence of a magnetic field showed that the mutants did not respond to magnetic fields of μT range. Although we did not measure the magnetic properties of the magnetosomes produced in *Magnetospirillum* sp. 15-1 directly, their small size (<25 nm) suggests that they are likely superparamagnetic and, thus, are not efficiently magnetized by the weak geomagnetic field. Together with the poor arrangement within the cells, this seems to lead to the lack of cell alignment under the tested conditions. The fields applied in the current research were ~8–12-fold stronger than the geomagnetic field, suggesting that the benefits of magnetotaxis as a navigation tool would not be used by the strain to the fullest extent in the natural environment. Although the source from which *Magnetospirillum* sp. 15-1 was isolated, represented a constructed wetland model system (planted fixed-bed reactor) devoid of chemical gradients by generating a

macro-gradient-free flow (Martínez-Lavanchy *et al.*, 2015), native wetlands form vertically stratified redox gradients, similar to aquatic sediments (Noll *et al.*, 2005). Therefore, they represent a type of environments in which magnetotaxis may provide an advantage.

Differences in the expression levels of at least several magnetosome proteins in comparison to MSR-1 could account for the weak magnetic phenotype in *Magnetospirillum* sp. 15-1. Western blot analysis of 11 magnetosome proteins in *Magnetospirillum* sp. 15-1 *tpsMAG* revealed somewhat imbalanced expression of magnetosome proteins. Thus, the expression of MamB and MamY was weaker, than for the other tested proteins. MamB is an essential protein for magnetosome biosynthesis due to its two important functions: initiation of MM vesicles formation and transport of ferrous iron into magnetosomes (Keren-Khadmy *et al.*, 2018). Therefore, relatively low abundance of MamB can explain small magnetite crystals in *Magnetospirillum* sp. 15-1. Very recently, MamY was demonstrated to determine the position of the magnetosome chain along the positive inner cell curvature of helically shaped MSR-1 cells (Toro-Nahuelpan *et al.*, 2019). It, therefore, seems plausible that insufficient synthesis of MamY in *Magnetospirillum* sp. 15-1 may be one of the reasons for the poor magnetosome arrangement. One explanation for the differences in the expression can be inadequate recognition of transcription regulatory elements, e.g. promoters and transcriptional regulators binding sites, by the new host. On the other hand, partial degradation of the heterologous proteins is also possible. Besides, we cannot rule out accumulation of point mutations or small indels in the cassette. The sequence of pTpsMAG1 was verified prior to transfer (data not shown); however, acquisition of such mutations could happen in the host after integration of the cassette into the chromosome.

Despite repeated attempts, we failed to transfer pTpsMAG1 into *M. aberrantis* and *M. bellicus*. Besides conjugation, various electroporation protocols were also tried in both strains with no positive result (data not shown). Further investigation on the possible reasons showed evidence for some mechanisms of self-protection against foreign DNA, likely a RM system, involved. Treatment of plasmid DNA isolated from *E. coli*, or even more closely related MSR-1, with cell extracts prepared from *M. aberrantis* and *M. bellicus* efficiently digested DNA, and analysis of genome sequences of the strains revealed the presence of several RM systems belonging to different types making it difficult to predict the one in action for each strain (Table S2). Considering the concurrent absence of the MAI in both strains, it seems reasonable that a putative RM system(s) might prevent *M. aberrantis* and *M. bellicus* from re-acquiring magnetosome genes by HGT. This may

generally represent a limiting factor for the horizontal expansion of magnetosome genes, even within groups of closely related species under natural environmental conditions.

In conclusion, we demonstrated that the single-step transfer of the known magnetosome operons from a freshwater sediment-dwelling magnetotactic strain MSR-1 to a non-magnetotactic wetland-inhabiting species of *Magnetospirillum* was sufficient to 'magnetize' the latter. The observed magnetosomes and inefficient magnetotaxis in relatively weak magnetic fields highlight the potential limitations in the ability of horizontally transferred genes to endow a new host with magnetotactic lifestyle. However, the ability of *Magnetospirillum* sp. 15-1 *tpsMAG* to respond to strong magnets, in combination with the capacity of the strain to degrade toluene and other aromatic compounds under anaerobic conditions (Meyer-Cifuentes *et al.*, 2017b), opens new possibilities to engineer magnetically controllable strains for bioremediation. In addition, we provide evidence for a putative RM system(s) in magnetospirilla that might represent a natural barrier for the horizontal expansion of magnetosome genes within the genus in their natural habitats. Overall, our findings will stimulate future attempts to reconstitute the magnetosome biomineralization in foreign non-magnetotactic organisms.

ACKNOWLEDGEMENTS

This project has received funding from the European Research Council (ERC) under the European Union's Horizon 2020 research and innovation program (Grant Agreement No. 692637 (to D.S.)). The work of MD was also partially supported by DAAD scholarship. The funders had no role in study design, data collection and interpretation, or the decision to submit the work for publication. We are grateful to Dr. Heipieper and I. Meyer-Cifuentes for providing us with the strain *Magnetospirillum* sp. 15-1. The authors thank Dr. M. Schüler and Prof. Dr. S. Geimer for help with TEM. We also thank Dr. D. Pfeiffer for help with swarm agar assay and video recording and I. Gild for technical assistance.

References

Abràmoff, M.D., Magalhães, P.J., and Ram, S.J. (2004) Image processing with imageJ. *Biophotonics Int* **11**: 36–42.

Bjerrum, O.J., and Schafer-Nielsen, C. (1986). In *Proceedings of the Fifth Meeting of the International Electrophoresis Society*, Dunn, M.J. (ed). VCH Verlagsgesellschaft: Weinheim, Germany, pp. 315–327.

Blakemore, R.P., Maratea, D., and Wolfe, R.S. (1979) Isolation and pure culture of a freshwater magnetic spirillum in chemically defined medium. *J Bacteriol* **140**: 720–729.

Borole, A.P., Mielenz, J.R., Vishnivetskaya, T.A., and Hamilton, C.Y. (2009) Controlling accumulation of

fermentation inhibitors in biorefinery recycle water using microbial fuel cells. *Biotechnol Biofuels* **2**: 7.

Bourceret, A., Leyval, C., Faure, P., Lorgeoux, C., and Cébron, A. (2018) High PAH degradation and activity of degrading bacteria during alfalfa growth where a contrasted active community developed in comparison to unplanted soil. *Environ Sci Pollut Res* **25**: 29556–29571.

Donahue, J.P., Israel, D.A., Peek, R.M., Blaser, M.J., and Miller, G.G. (2000) Overcoming the restriction barrier to plasmid transformation of *Helicobacter pylori*. *Mol Microbiol* **37**: 1066–1074.

Dziuba, M., Koziaeva, V., Grouzdev, D., Burganskaya, E., Baslerov, R., Kolganova, T., *et al.* (2016) *Magnetospirillum caucaseum* sp. nov., *Magnetospirillum marisnigri* sp. nov. and *Magnetospirillum moscoviense* sp. nov., freshwater magnetotactic bacteria isolated from three distinct geographical locations in European Russia. *Int J Syst Evol Microbiol* **66**: 2069–2077.

Dzyuba, M.V., Mardanov, A.V., Beletskii, A.V., Kolganova, T. V., Sukhacheva, M.V., Shelonkov, A.A., *et al.* (2012) Reconstruction of iron metabolism pathways of bacteria *Magnetospirillum aberrantis* SpK spp. based on sequenced genome analysis. *Dokl Biol Sci* **444**: 335–338.

Fling, S.P., and Gregerson, D.S. (1986) Peptide and protein molecular weight determination by electrophoresis using a high-molarity tris buffer system without urea. *Anal Biochem* **15**: 83–88.

Frankel, R.B., Blakemore, R.P., and Wolfe, R.S. (1979) Magnetite in freshwater magnetotactic bacteria. *Science* **203**: 1355–1356.

Fukuda, Y., Okamura, Y., Takeyama, H., and Matsunaga, T. (2006) Dynamic analysis of a genomic Island in *Magnetospirillum* sp. strain AMB-1 reveals how magnetosome synthesis developed. *FEBS Lett* **580**: 801–812.

Gorlenko, V.M., Dzyuba, M.V., Maleeva, A.N., Panteleeva, A. N., Kolganova, T.V., and Kuznetsov, B.B. (2011) *Magnetospirillum aberrantis* sp. nov., a new freshwater bacterium with magnetic inclusions. *Microbiology* **80**: 692.

Heyen, U., and Schüler, D. (2003) Growth and magnetosome formation by microaerophilic *Magnetospirillum* strains in an oxygen-controlled fermentor. *Appl Microbiol Biotechnol* **61**: 536–544.

Kalyaanamoorthy, S., Minh, B.Q., Wong, T.K.F., Von Haeseler, A., and Jermini, L.S. (2017) ModelFinder: fast model selection for accurate phylogenetic estimates. *Nat Methods* **14**: 587–589.

Katzmann, E., Scheffel, A., Gruska, M., Plietzko, J.M., and Schüler, D. (2010) Loss of the actin-like protein MamK has pleiotropic effects on magnetosome formation and chain assembly in *Magnetospirillum gryphiswaldense*. *Mol Microbiol* **77**: 208–224.

Ke, L., Chen, Y., Liu, P., Liu, S., Wu, D., Yuan, Y., *et al.* (2018) Characteristics and optimised fermentation of a novel magnetotactic bacterium, *Magnetospirillum* sp. ME-1. *FEMS Microbiol Lett* **365**: fny052.

Keren-Khadmy, N., Zeytuni, N., Katzmann, E., Navon, Y., Davidov, G., Plietzko, M., and Sch, D. (2018) The dual role of MamB in magnetosome membrane assembly and magnetite biomineralization. *Mol Microbiol* **107**: 542–557.

- Kolinko, I., Jogler, C., Katzmann, E., and Schüler, D. (2011) Frequent mutations within the genomic magnetosome island of *Magnetospirillum gryphiswaldense* are mediated by RecA. *J Bacteriol* **193**: 5328–5334.
- Kolinko, I., Lohße, A., Borg, S., Raschdorf, O., Jogler, C., Tu, Q., *et al.* (2014) Biosynthesis of magnetic nanostructures in a foreign organism by transfer of bacterial magnetosome gene clusters. *Nat Nanotechnol* **9**: 193–197.
- Komeili, A. (2012) Molecular mechanisms of compartmentalization and biomineralization in magnetotactic bacteria. *FEMS Microbiol Rev* **36**: 232–255.
- Koziaeva, V.V., Dziuba, M.V., Ivanov, T.M., Kuznetsov, B.B., Skryabin, K.G., and Grouzdev, D.S. (2016) Draft genome sequences of two magnetotactic bacteria, *Magnetospirillum moscoviense* BB-1 and *Magnetospirillum marisnigri* SP-1. *Genome Announc* **4**: e00814–e00816.
- Koziaeva, V.V., Rusakova, S.A., Slobodova, N.V., Uzun, M., Kolganova, T.V., Skryabin, K.G., and Grouzdev, D.S. (2019) *Magnetospirillum kuznetsovii* sp. nov., a novel magnetotactic bacterium isolated from a lake in the Moscow region. *Int J Syst Evol Microbiol* **69**: 1953–1959.
- Ladner, C.L., Yang, J., Turner, R.J., and Edwards, R.A. (2004) Visible fluorescent detection of proteins in polyacrylamide gels without staining. *Anal Biochem* **326**: 13–20.
- Lahme, S., Trautwein, K., Strijkstra, A., Dorries, M., Wohlbrand, L., and Rabus, R. (2014) Benzoate mediates the simultaneous repression of anaerobic 4-methylbenzoate and succinate utilization in *Magnetospirillum* sp. strain pMbN1. *BMC Microbiol* **14**: 269.
- Lefevre, C.T., Schmidt, M.L., Vioria, N., Trubitsyn, D., Schüler, D., and Bazylinski, D.A. (2012) Insight into the evolution of magnetotaxis in *Magnetospirillum* spp., based on mam gene phylogeny. *Appl Environ Microbiol* **78**: 7238–7248.
- Letunic, I., and Bork, P. (2019) Interactive tree of life (iTOL) v4: recent updates and new developments. *Nucleic Acids Res* **47**: W256–W259.
- Li, Y., Bali, S., Borg, S., Katzmann, E., Ferguson, S.J., and Schüler, D. (2013) Cytochrome cd1 nitrite reductase NirS is involved in anaerobic magnetite biomineralization in *Magnetospirillum gryphiswaldense* and requires nirM for proper d1 heme assembly. *J Bacteriol* **195**: 4297–4309.
- Li, Y., Katzmann, E., Borg, S., and Schüler, D. (2012) The periplasmic nitrate reductase nap is required for anaerobic growth and involved in redox control of magnetite biomineralization in *Magnetospirillum gryphiswaldense*. *J Bacteriol* **194**: 4847–4856.
- Lin, W., Wang, Y., Gorby, Y., Nealson, K., and Pan, Y. (2013) Integrating niche-based process and spatial process in biogeography of magnetotactic bacteria. *Sci Rep* **3**: 1643.
- Lohße, A., Kolinko, I., Raschdorf, O., Uebe, R., Borg, S., Brachmann, A., *et al.* (2016) Overproduction of magnetosomes by genomic amplification of biosynthesis-related gene clusters in a magnetotactic bacterium. *Appl Environ Microbiol* **82**: 3032–3041.
- Lohße, A., Ullrich, S., Katzmann, E., Borg, S., Wanner, G., Richter, M., *et al.* (2011) Functional analysis of the magnetosome island in *Magnetospirillum gryphiswaldense*: the mamAB operon is sufficient for magnetite biomineralization. *PLoS One* **6**: e25561.
- Lu, Y., Rosencrantz, D., Liesack, W., and Conrad, R. (2006) Structure and activity of bacterial community inhabiting rice roots and the rhizosphere. *Environ Microbiol* **8**: 1351–1360.
- Maratea, D., and Blakemore, R.P. (1981) *Aquaspirillum magnetotacticum* sp. nov., a magnetic spirillum. *Int J Syst Bacteriol* **31**: 452–455.
- Martínez-Lavanchy, P.M., Chen, Z., Lünsmann, V., Marin-Cevada, V., Vilchez-Vargas, R., Pieper, D.H., *et al.* (2015) Microbial toluene removal in hypoxic model constructed wetlands occurs predominantly via the ring monooxygenation pathway. *Appl Environ Microbiol* **81**: 6241–6252.
- Matsunaga, T., Okamura, Y., Fukuda, Y., Wahyudi, A.T., Murase, Y., and Takeyama, H. (2005) Complete genome sequence of the facultative anaerobic magnetotactic bacterium *Magnetospirillum* sp. strain AMB-1. *DNA Res* **12**: 157–166.
- Matsunaga, T., Sakaguchi, T., and Tadakoro, F. (1991) Magnetite formation by a magnetic bacterium capable of growing aerobically. *Appl Microbiol Biotechnol* **35**: 651–655.
- Mediavilla, O., Geml, J., Olaizola, J., Oria-de-Rueda, J.A., Baldrian, P., and Martín-Pinto, P. (2019) Effect of forest fire prevention treatments on bacterial communities associated with productive *Boletus edulis* sites. *J Microbiol Biotechnol* **12**: 1188–1198.
- Meyer-Cifuentes, I., Fiedler, S., Müller, J.A., Kappelmeyer, U., Mäusezahl, I., and Heipieper, H.J. (2017a) Draft genome sequence of *Magnetospirillum* sp. strain 15-1, a denitrifying toluene degrader isolated from a planted fixed-bed reactor ingrid. *Genome Announc* **5**: 20–21.
- Meyer-Cifuentes, I., Martínez-Lavanchy, P.M., Marin-Cevada, V., Böhnke, S., Harms, H., Müller, J.A., and Heipieper, H.J. (2017b) Isolation and characterization of *Magnetospirillum* sp. strain 15-1 as a representative anaerobic toluene-degrader from a constructed wetland model. *PLoS One* **12**: 1–16.
- Nguyen, L.T., Schmidt, H.A., Von Haeseler, A., and Minh, B. Q. (2015) IQ-TREE: A fast and effective stochastic algorithm for estimating maximum-likelihood phylogenies. *Mol Biol Evol* **32**: 268–274.
- Noll, M., Matthies, D., Frenzel, P., Derakshani, M., and Liesack, W. (2005) Succession of bacterial community structure and diversity in a paddy soil oxygen gradient. *Environ Microbiol* **7**: 382–395.
- Popp, F., Armitage, J.P., and Schüler, D. (2014) Polarity of bacterial magnetotaxis is controlled by aerotaxis through a common sensory pathway. *Nat Commun* **14**: 5398.
- Raschdorf, O., Bonn, F., Zeytuni, N., Zarivach, R., Becher, D., and Schüler, D. (2018a) A quantitative assessment of the membrane-integral sub-proteome of a bacterial magnetic organelle. *J Proteomics* **172**: 89–99.
- Raschdorf, O., Plitzko, J.M., Schüler, D., and Müller, F.D. (2014) A tailored galK counterselection system for efficient markerless gene deletion and chromosomal tagging in *Magnetospirillum gryphiswaldense*. *Appl Environ Microbiol* **80**: 4323–4330.

- Raschdorf, O., Schüler, D., and Uebe, R. (2018b) Preparation of bacterial magnetosomes for proteome analysis. In *Microbial Proteomics: Methods and Protocols*, Becher, D. (ed). New York, NY: Springer, pp. 45–57.
- Rioux, J.B., Philippe, N., Pereira, S., Pignol, D., Wu, L.F., and Ginet, N. (2010) A second actin-like mamK protein in *Magnetospirillum magneticum* AMB-1 encoded outside the genomic magnetosome island. *PLoS One* **5**: e9151.
- Sambrook, J., and Russell, D.W. (2001) *Molecular Cloning: A Laboratory Manual*, 3rd ed. Cold Spring Harbor, New York: Cold Spring Harbor Laboratory Press.
- Scheffel, A., and Schüler, D. (2007) The acidic repetitive domain of the *Magnetospirillum gryphiswaldense* MamJ protein displays hypervariability but is not required for magnetosome chain assembly. *J Bacteriol* **189**: 6437–6446.
- Schleifer, K.H., Schüler, D., Spring, S., Weizenegger, M., Amann, R., Ludwig, W., and Köhler, M. (1991) The genus *Magnetospirillum* gen. nov. description of *Magnetospirillum gryphiswaldense* sp. nov. and transfer of *Aquaspirillum magnetotacticum* to *Magnetospirillum magnetotacticum* comb. nov. *Syst Appl Microbiol* **14**: 379–385.
- Schübbe, S., Kube, M., Scheffel, A., Wawer, C., Heyen, U., Meyerdierks, A., et al. (2003) Characterization of a spontaneous nonmagnetic mutant of *Magnetospirillum gryphiswaldense* reveals a large deletion comprising a putative magnetosome island. *J Bacteriol* **185**: 5779–5790.
- Schüler, D., and Köhler, M. (1992) The isolation of a new magnetic spirillum. *Zentralbl Mikrobiol* **147**: 150–151.
- Schüler, D., Spring, S., and Bazylinski, D.A. (1999) Improved technique for the isolation of magnetotactic spirilla from a freshwater sediment and their phylogenetic characterization. *Syst Appl Microbiol* **22**: 466–471.
- Schüler, D., Uhl, R., and Bäuerlein, E. (1995) A simple light scattering method to assay magnetism in *Magnetospirillum gryphiswaldense*. *FEMS Microbiol Lett* **132**: 139–145.
- Schultheiss, D., and Schüler, D. (2003) Development of a genetic system for *Magnetospirillum gryphiswaldense*. *Arch Microbiol* **179**: 89–94.
- Shinoda, Y., Akagi, J., Uchihashi, Y., Hiraishi, A., Yukawa, H., Yurimoto, H., et al. (2005) Anaerobic degradation of aromatic compounds by *Magnetospirillum* strains: isolation and degradation genes. *Biosci Biotechnol Biochem* **69**: 1483–1491.
- Shinoda, Y., Sakai, Y., Ué, M., Hiraishi, A., and Kato, N. (2000) Isolation and characterization of a new denitrifying spirillum capable of anaerobic degradation of phenol. *Appl Environ Microbiol* **66**: 1286–1291.
- Smalley, M.D., Marinov, G.K., Bertani, L.E., and DeSalvo, G. (2016) Genome sequence of *Magnetospirillum magnetotacticum* strain MS-1. *Genome Announc* **3**: 10–11.
- Thrash, J.C., Ahmadi, S., Torok, T., and Coates, J.D. (2010) *Magnetospirillum bellicus* sp. nov., a novel dissimilatory perchlorate-reducing alphaproteobacterium isolated from a bioelectrical reactor. *Appl Environ Microbiol* **76**: 4730–4737.
- Torella, J.P., Lienert, F., Boehm, C.R., Chen, J., Way, J.C., and Silver, P.A. (2014) Unique nucleotide sequence-guided assembly of repetitive DNA parts for synthetic biology applications. *Nat Protoc* **9**: 2075–2089.
- Toro-Nahuelpan, M., Giacomelli, G., Raschdorf, O., Borg, S., Plietzko, J.M., Bramkamp, M., et al. (2019) MamY is a membrane-bound protein that aligns magnetosomes and the motility axis of helical magnetotactic bacteria. *Nat Microbiol* **4**: 1978–1989.
- Uebe, R., and Schüler, D. (2016) Magnetosome biogenesis in magnetotactic bacteria. *Nat Rev Microbiol* **14**: 621–637.
- van der Lelie, D., Taghavi, S., McCorkle, S.M., Li, L.L., Malfatti, S.A., Monteleone, D., et al. (2012) The metagenome of an anaerobic microbial community decomposing poplar wood chips. *PLoS One* **7**: e36740.
- Wang, J., Sarov, M., Rientjes, J., Fu, J., Hollak, H., Kranz, H., et al. (2006) An improved recombineering approach by adding RecA to λ red recombination. *Mol Biotechnol* **32**: 43–53.
- Wang, Y., Lin, W., Li, J., Zhang, T., Li, Y., Tian, J., et al. (2015) Characterizing and optimizing magnetosome production of *Magnetospirillum* sp. XM-1 isolated from Xi'an City moat, China. *FEMS Microbiol Lett* **362**: 1–8.
- Yin, H., Niu, J., Ren, Y., Cong, J., Zhang, X., Fan, F., et al. (2015) An integrated insight into the response of sedimentary microbial communities to heavy metal contamination. *Sci Rep* **22**: 14266.

Supporting Information

Additional Supporting Information may be found in the online version of this article at the publisher's web-site:

Movie S1. Swimming behaviour of *M. gryphiswaldense* in the absence of the applied magnetic field*. Note the random movement of the cells.

Movie S2. Swimming behaviour of *M. gryphiswaldense* in the magnetic field of 400 μ T directed along the X axis.

Movie S3. Swimming behaviour of *M. gryphiswaldense* in the magnetic field of 400 μ T directed along the Y axis

Movie S4. Swimming behaviour of *Magnetospirillum* sp. 15–1 *tpsMAG* in the absence of the applied magnetic field.

Movie S5. Swimming behavior of *Magnetospirillum* sp. 15–1 *tpsMAG* in the magnetic field of 400 μ T directed along the X axis.

Movie S6. Swimming behaviour of *Magnetospirillum* sp. 15–1 *tpsMAG* in the magnetic field of 400 μ T directed along the Y axis *Geomagnetic field was not compensated in all experiments

Table S1. Oligonucleotides used in the study

Table S2. Annotated genes for potential restrictases belonging to various restriction-modification systems in the genomes of *M. bellicus* VDY and *M. aberrantis* SpK

Fig. S1. PCR-test for the integrity of the magnetosome gene expression cassette in *Magnetospirillum* sp. 15–1 mutants. The PCR fragments cover different regions of the transferred magnetosome operons. (M) marker, (+) plasmid pTpsMAG1 was used as positive control, wild type strain was used as negative control. The selected mutants are highlighted by red circles.

Fig. S2. Effect of anaerobic nitrate respiration on magnetosome biomineralization in *Magnetospirillum* sp. 15–1. (A) Cultivation in FSM medium with 0.2% agar and 8 mM NaNO₃ shows microaerophilic band (white arrow head) and nitrogen bubbles (green arrow) as indication of the activity of dissimilatory nitrate reduction pathway.

(B) Effect of different nitrate concentrations on Cmag (i), magnetosome diameter (ii) and number (iii) in *Magnetospirillum* sp. 15–1 *tpsMAG* C5 under anaerobic conditions. (C) TEM micrographs with exemplary cells demonstrating magnetosomes in the cells grown with different nitrate concentrations under anaerobic conditions.